Structural, dielectric and ferroelectric properties of (Bi,Na)TiO_3-$BaTiO_3$ system studied by high throughput screening

Brian E. Hayden,[a,b] and Sergey Yakovlev[a,*]

[a]*Ilika Technologies Plc., Kenneth Dibben House, Enterprise Road, University of Southampton Science Park, Chilworth, Southampton, SO16 7NS, UK*

[b]*Department of Chemistry, University of Southampton, Highfield, Southampton, SO17 1BJ, UK*

Abstract

Thin-film materials libraries of the Bi_2O_3-Na_2O-TiO_2-BaO system in a broad composition range have been deposited in ultra-high vacuum from elemental evaporation sources and an oxygen plasma source. A high throughput approach was used for systematic compositional and structural characterization and the screening of the dielectric and ferroelectric properties. The perovskite (Bi,Na)TiO_3-$BaTiO_3$ phase with a Ba concentration near the morphotropic phase boundary (ca. 6 At. %) exhibited a relative dielectric permittivity of 180, a loss tangent of 0.04 and remnant polarization of 19 μC/cm^2. Compared to published data, observed remnant polarization is close to that known for epitaxially grown films but higher than the values reported for polycrystalline films. The high throughput methodology and systematic nature of the study allowed us to establish the composition boundaries of the phase with optimal dielectric and ferroelectric characteristics.

Keywords: lead-free piezoelectric; high-throughput screening; PVD; ferroelectric thin films; perovskite

* Corresponding author: Tel.: +44 2380111400; fax: +44 2380111400.

E-mail address: sergey.yakovlev@ilika.com (Sergey Yakovlev).

1. Introduction

Due to the environmental concerns, considerable efforts have been focused for the last decade on replacing lead-zirconate-titanate (PZT) ferroelectric system, presently dominating the field of electromechanical actuators and sensors, with lead-free compounds. Trends and achievements in this area have been summarized in several comprehensive reviews [1-8]. $(Bi_{0.5}Na_{0.5})TiO_3$-$BaTiO_3$ (BNT-BT) is the pseudo-binary system of perovskite-type solid solutions which is drawing a particular attention (see, e.g. ref.'s 8-10 and references cited therein) due to promising piezoelectric and ferroelectric properties. At room temperature, $BaTiO_3$ and $(Bi_{0.5}Na_{0.5})TiO_3$ have tetragonal and rhombohedral crystal structures, respectively. It was reported that these compounds form a morphotropic phase boundary (MPB) around 6-7 mol. % of $BaTiO_3$ [9,10] (both, molar (mol.) and atomic (At.) percent will be used in this work to denote composition). By analogy with the well-studied PZT system, MPB compounds in the BNT-BT system are expected to demonstrate dielectric, ferroelectric and electromechanical properties superior to those of the end compounds [4,5,7,8-10].

In this work, we used a high throughput physical vapour deposition (HT-PVD) technique to synthesise libraries of Bi-Na-Ti-Ba-O thin films. Combinatorial screening involving various processing techniques has been proven to be an indispensable tool for accelerated discovery of multicomponent functional materials [11]. The HT-PVD method employed here is based on the simultaneous deposition of elements from MBE (Knudsen cell or e-beam evaporator) and a plasma atom source on an appropriate substrate [12]. The composition gradients of the elements across a substrate in the target range are controllable and are achieved using a "wedge" shutter on each source [12] and this method has been successfully applied to the synthesis and screening of ferroelectric perovskite [13,14], and tuneable pyrochlore [15,16] thin films.

In our recent work, we employed HT-PVD approach to synthesise thin-film libraries of compounds in the Bi_2O_3-TiO_2-Na_2O pseudo-ternary system and studied their structural and dielectric and ferroelectric properties [13]. This system, in particular, contains well-known $Bi_{0.5}Na_{0.5}TiO_3$ perovskite-type ferroelectric compound. It was found that dielectric and ferroelectric properties of the BNT are very sensitive to the deviation from the nominal cationic stoichiometry and the composition boundaries of an existence of the phase with high ferroelectric response have been established. As an expansion of this work, in this paper we report the results of HT-PVD synthesis and screening of the structural and dielectric and ferroelectric

properties of the Bi_2O_3-Na_2O-TiO_2-BaO thin-film materials libraries in a broad range of compositions. Particular emphasis is put on composition boundaries of formation of perovskite phase in the system and effect of composition on the dielectric and ferroelectric properties.

2. Experimental

Bi-Na-Ti-Ba-O polycrystalline thin-film materials libraries were synthesized in a modified PVD system from DCA Instruments. Detailed description of the high throughput deposition method can be found elsewhere [12]. The thin films were fabricated on square 35×35 mm^2 silicon or platinized silicon substrates from Nova Electronic Materials. Samples for structural and electrical characterization were deposited on Si<100>/SiO_2(1000 nm)/TiO_2(20 nm)/Pt<111>(100 nm) substrates. Films used for composition and thickness measurements were processed on Si<100> substrates. Prior to deposition, substrates were cleaned in an ultrasonic bath for 10 min in 50% solution of ethanol absolute in deionized water and 10 min in iso-propanol absolute. After cleaning, the substrates were dried in a flow of nitrogen. Deposition of thin films was carried out in a cryo-pumped ultra-high vacuum (UHV) environment. Individual off-axis sources with associated wedge shutters [12] were used to deposit continuous thin films with a broad composition gradient across the substrate. Na (99.9 %, Aldrich), Ba (99.2 %, Alfa-Aesar) and Bi (99.999 %, Alfa-Aesar) were evaporated using Knudsen cells; Ti (99.995%, Alfa Aesar) was deposited from the electron-beam source. Quartz crystal micro-balances were used to monitor the deposition rates of individual elements. Oxygen was incorporated using a plasma source with a discharge power of 600 W and an oxygen flow rate 5 sccm. The wedge positions and deposition rates were optimized during processing of the films to obtain material with a composition within the desired range.

The elemental composition of the films was measured on 14×14 arrays of locations on a substrate by inductively coupled plasma mass spectrometry (ICP-MS, Perkin-Elmer ELAN 9000 mass spectrometer equipped with the New Wave Research UP213 laser ablation system). Helium was used as a carrier gas. In order to achieve a suitable composition spread, the deposition conditions were adjusted using materials libraries deposited for 30 min. This deposition time resulted in thin films with a thickness of 80-120 nm. Thickness variation is inevitable in the thin-film materials libraries due to chemical composition gradient across a substrate. In order to study the electrical properties of the thin films, another library was deposited under optimized conditions for 1 hour, resulting in a thickness 160-240 nm. Fig. 1 shows the composition

range of this materials library on a typical chip. For ease of presentation and interpretation, rather than plotting data as a function of composition in a quaternary "pyramid", we have reduced quaternary representation to pseudo-ternary plots by combining either the Bi and Na concentrations (Fig. 2a) or the Ba and Ti concentrations (Fig. 2b). Phase composition of the films was analysed for a 14×14 matrix of locations using the Brucker D8 Discover X-ray Diffractometer system incorporating a HI Star area detector, IμS Incoatec Microfocus Cu Kα source with a UMC 150 sample stage. The thickness of the films was determined using the Veeco MYKO NT1100 optical profiling system. Samples for thickness measurements were deposited on Si<100> substrates through the contact mask with 14×14 mesh of square holes and then capped by the 20 nm continuous layer of Cu in an RF sputterer to achieve uniform reflectivity across the sample. All samples were found to have 20-33 % thickness gradient due to composition non-uniformity. Electrical measurements were performed in a plane-capacitor configuration. An array of 19×19 Pt top electrodes with the diameter 0.25 mm were deposited by DC sputtering. A Hewlett-Packard 4284 LCR meter was used to measure relative permittivity, ε_r, and the loss tangent, tanδ, of the films. Polarization-voltage (*P-V*) hysteresis loops were acquired using a Precision RT66B Ferroelectric Tester from Radiant Technologies Inc. Automated sample positioning during dielectric and ferroelectric tests was performed using Signatone high-precision probe station. Data visualization and handling, including X-ray peak area calculation, was performed using a proprietary informatics software suite.

3. Results and discussion

3.1. Screening of the perovskite phase formation in the Bi-Na-Ti-Ba-O thin-film materials library

In an attempt to crystallise materials *in situ*, thin films were deposited at various substrate temperatures ranging from 400 °C to 700 °C. We have found that at the substrate temperature as low as 400 °C, Na and Bi do not effectively incorporate in the thin film due to re-evaporation from the substrate during deposition. Therefore, all subsequent depositions were conducted without heating followed by post-deposition annealing in a tube furnace at 700 °C for 30 min in oxygen flow to induce crystallization. Structural and electrical characterization showed that this procedure results in high-quality materials libraries. Pt top electrodes for electrical measurements were sputtered prior to annealing. The composition was measured on the annealed films.

Fig. 3 shows the results of screening of the formation of perovskite phase in the Bi-Na-Ti-Ba-O library deposited for 1 hour and annealed at 700 °C for 30 min in oxygen (thickness of the films ranges from 160 to 240 nm). Fig. 3a shows the on-chip distribution of the area under (110) perovskite peak. Due to proximity of crystal structures of $(Bi,Na)TiO_3$ and $BaTiO_3$, rhombohedral and tetragonal phases could not be resolved in X-ray diffraction experiments on thin films and therefore a pseudo-cubic notation is used throughout the paper. Fig. 3b shows exemplarily the XRD pattern corresponding to the composition with nearly equimolar Bi/Na ratio and Ba content close to the MPB. The XRD analysis confirms crystallization of the perovskite phase in the composition range of interest thus indicating the suitability of proposed processing method and the post-deposition thermal treatment. Dependence of the area under the (110) perovskite peak on the composition (in pseudo-ternary composition space) is shown on Fig. 3c,d. It can be seen that the data points with the largest area of the (110) peak is observed for the composition range around 50 at. % of Ti. With respect to Bi and Na content, the perovskite phase is found to exist in a broad range, which apparently expands into compositions beyond the sample boundaries. This is also evident from Fig. 3a. Sorting out XRD patterns describing pure perovskite (no reflections or traces of other phases) was performed manually. This manual data discrimination allowed to unambiguously determine the boundaries of an existence of pure perovskite phase in the system (within the sensitivity of the diffractometer). The results are presented on Fig. 3e,f in pseudo-ternary composition space. These findings can be used as a guideline for the stoichiometry adjustment during materials processing. Outside the “pure perovskite” region, as expected, X-ray diffractometry revealed rather complicated overall phase composition due to a very large number of combinations of stoichiometries and broad range of compositions within a single materials library. The influence of secondary phases on the ferroelectric and dielectric properties of the perovskite $(Bi,Na)TiO_3$-$BaTiO_3$ solid solutions will be discussed in section 3.3.

3.2. Dielectric properties

Fig. 4 shows the room-temperature relative permittivity of the Bi-Na-Ti-Ba-O thin-film materials library on chip (a) and as a function of composition (b,c). The data were acquired at a frequency 1 kHz and peak-to-peak voltage amplitude of 50 mV. Cross symbols on Fig. 4a mark defect electrodes which could not be measured due to their poor mechanical integrity: these electrodes partially exfoliated from the sample in the course of annealing. Interestingly, this electrode failure effect is of systematic nature and reflects

variation of adhesion of sputtered Pt electrode layer as a function of phase and elemental composition. Identical effect was observed in our previous work on Bi_2O_3-Na_2O-TiO_2 system (see ref. 13 for more details).

Optimized deposition conditions resulted in high-quality films with maximum relative permittivity of 180 and loss tangent 0.04 observed for the composition near the MPB (position of the MPB compound in the composition space is marked for the reference on Fig. 3e). Very important observation was made for the dependence of the ε_r on the titanium content: it can be seen that relative permittivity forms a distinct compositional boundary where it drops abruptly. This effect is seen clearly on Fig. 4a. The boundary lies within the region of existence of the perovskite phase and coincides with the "edge" of the pure perovskite area (dashed lines on Fig. 4b,c). Increasing titanium content above 50 At. % produces gradual, rather than abrupt decreasing in ε_r. This behaviour could only be studied systematically due to continuous composition variation in the thin-film materials library. In bulk $(Na_{0.5}Bi_{0.5})TiO_3$ ceramics, the effects of small stoichiometry variations were systematically investigated by Li *et al.* [17]. In this work, bismuth excess and deficiency as low as 1 mol. % were introduced during materials processing and electronic and oxygen-ionic transport properties of ceramics were studied vs. temperature. It was found that the material undergoes pronounced insulator-to-conductor transition with decreasing bismuth content from 51 to 49 mol. % with associated drop of the bulk resistivity by 3-4 orders of magnitude and near 50 % decrease of the activation energy of conductivity. It is clear from our work that at room temperature electronic conductivity is very sensitive to both Na and Bi deficiency with respect to Ti. Such a dramatic change of type of the conductivity within very narrow range of compositions clearly demonstrates necessity of precise composition control during materials processing and also explains significant scatter in published dielectric and ferroelectric data (see following section).

3.3. Ferroelectric properties

Several regions of the following types of *P-V* responses were identified within the studied thin-film materials library: ferroelectric, linear dielectric, lossy dielectric and "no contact". Classification and locations of these regions on-chip and in composition space is shown on Fig. 5. Fig. 5a shows classification of *P-V* characteristics on chip. Only the fragment of the materials library encompassing the ferroelectric phases is relevant to the following discussion. It is convenient to show both ferroelectric and dielectric data on one

image: Fig. 5a compares on-chip distribution of the relative dielectric permittivity (Fig. 4a, section 3.2) and classification of ferroelectric responses. The dashed lines delineate the region of the sample corresponding to the ferroelectric data. Two points in this region could not be measured due to mechanically damaged Pt top contacts. These points are indicated as "no contact". Fig. 5b,c shows locations of ferroelectric and linear fields on pseudo-ternary plots; lossy and "no contact" types of the data are not included for clarity. Fig. 6 shows the *P-V* characteristics obtained for representative compounds from ferroelectric and linear areas. It is important to point out that the observed ferroelectric responses could be classified as two different limits, denoted as "Ferro-1" and "Ferro-2". These two areas demonstrated distinct types of *P-V* hysteresis loops. *P-V* characteristics obtained for the second ferroelectric phase showed non-saturated (or incipient) hysteresis loop with very low spontaneous polarization, Fig. 6b. The results, however, show a distinction from the linear dielectric (Fig. 6a) or lossy dielectric behaviour, and these materials can nevertheless be regarded as ferroelectric. It can be seen on Fig. 5b,c that the "Ferro-1" range forms two boundaries in the composition space: with the "Ferro-2" and linear areas. At the "Ferro-1"-linear boundary, remnant and spontaneous polarizations undergo a gradual decrease with lowering Ba content, as shown schematically on Fig. 5b (dashed line). The observed trend is in complete agreement with the results reported for (1-x)($Bi_{0.5}Na_{0.5}$)TiO_3-x$BaTiO_3$ (x=0.00-0.007) ceramics [9]. It must be mentioned, however, that our films exhibited higher remnant polarization (compare 16.4 μC/cm^2 for ceramics with 7 mol. % of Ba [9] with 19.0 μC/cm^2 reported in this work for 6.6 mol. % of Ba, Fig. 6a). Ferroelectric properties of polycrystalline BNT-BT films near the MPB processed via PVD in this work are close to those reported for epitaxial films on MgO substrates ($P_r \approx 20$ μC/cm^2) [18] but significantly superior to polycrystalline thin films deposited by chemical solution [19-21] methods.

At the "Ferro-1"-"Ferro-2" boundary, in contrast, a stepwise transformation (the trend in P_r is shown schematically on Fig. 5b) of the *P-V* hysteresis occurs when the composition changes in the direction indicated by the solid arrow. Importantly, this sharp transition is congruent with the boundary of the area of high relative dielectric permittivity; the effect is clearly visualized on Fig. 5a (compare also Fig's 4b and 5b). In order to understand the effect of phase content on ferroelectric and dielectric properties of (Bi,Na)TiO_3-$BaTiO_3$ compounds in the materials library, X-ray diffraction patterns obtained for the linear, "Ferro-1" and "Ferro-2" phases were compared. Fig. 7 shows XRD patterns representative of these regions. Table on Fig. 7 lists compositions in At.%. For the linear and "Ferro-1" phases, pure perovskite was formed. With increasing

Bi and decreasing Ti contents, broad shoulder between 27 and 31° 2Θ appears in addition to the reflections from the perovskite phase. This indicates the evolution of a poorly crystallized or even amorphous second phase(s). Furthermore, this pattern also contains reflection at 27.7° 2Θ not accounted by the perovskite phase. It is not possible to identify second phases in the system from these data. Based on composition variations (see table on Fig. 7), we may speculate that formation of bismuth oxide occurs due to the bismuth excess and titanium deficiency. From the XRD data presented on Fig. 7 one can see that even outside the "pure perovskite" area (for the compositions covered by presented XRD data), the perovskite remains the dominant phase. However, formation of even small amounts of a second phase(s) produce dramatic effect on dielectric and ferroelectric responses, as illustrated on Fig's 4 and 5. According to Fig. 5b, "Ferro-1"-to-"Ferro-2" transition occurs when Ti content decreases to 49 at. % with simultaneous increasing of Bi.

Finally, based on ferroelectric properties obtained for compounds of appropriate compositions, we conclude that proposed method of deposition from the individual sources of elements is highly effective for the processing complex functional thin films with the characteristics close to those of "epitaxial" materials. It must also be mentioned that during composition optimization of compounds such as BNT-BT (with strong composition-property correlation) it is advantageous to be able to control deposition rates of the individual constituent elements rather than rely on a single source with complex stoichiometry (e.g. sputtering techniques).

4. Conclusions

A combinatorial physical vapour deposition method employing MBE evaporation sources of individual elements and oxygen plasma source was used to synthesize polycrystalline thin-film materials library of the Bi_2O_3-Na_2O-TiO_2-BaO system. The library enclosed, in particular, ferroelectric perovskite (Bi,Na)TiO_3-$BaTiO_3$ compound with the compositions around the MPB. High throughput X-ray diffractometry and dielectric and ferroelectric characterization methods were used for screening structural properties, dielectric permittivity and ferroelectric response of the representative materials library. Optimized conditions of post-deposition annealing (700 °C, 30 min in oxygen flow) resulted in a formation of perovskite phase and its composition boundaries have been established. It was found that perovskite BNT-BT phase can tolerate significant (several At. %) deficiency of A-site cations relative to B-site cations; yet minor deficiency of B-site cations (Ti) results in multi-phase compounds. Maximum relative permittivity of

180 and the remnant polarization of 19 μC/cm^2 were found for the compositions around MPB. Continuous, rather than sampled nature of the composition variation enabled us to study with precision dependencies of the dielectric and ferroelectric properties on the composition. The results presented in this work can be used as a guideline for properties and composition adjustment during materials processing.

Acknowledgement

Authors thank Dr. M.S.B. Darby for his assistance during sample preparation and ferroelectric characterization.

References

[1] E. Cross, Lead-free at last, Nature 432 (2004) 24.

[2] Y. Saito, H. Takao, T. Tani, T. Nonoyama, K. Takatori, T. Homma, T. Nagaya, M. Nakamura, Lead-free piezoceramics, Nature 432 (2004) 84.

[3] M. Demartin Maeder, D. Damjanovic, N. Setter, Lead free piezoelectric materials, J. Electroceram. 13 (2004) 385.

[4] T. Takenaka, H. Nagata, Y. Hiruma, Y. Yoshii, K. Matumoto, Lead-free piezoelectric ceramics based on perovskite structures, J. Electroceram. 19 (2007) 259.

[5] T. Takenaka, H. Nagata, Current status and prospects of lead-free piezoelectric ceramics, J. Eur. Ceram. Soc. 25 (2005) 2693.

[6] S. Zhang, T.R. Shrout, Lead-free piezoelectric ceramics vs. PZT? J. Electroceram. 19 (2007) 251.

[7] J. Rödel, W. Jo, K.T.P. Seifert, E.-M. Anton, T. Granzow, D. Damjanovic, Perspective on the development of lead-free piezoceramics, J. Am. Ceram. Soc. 92 (2009) 1153.

[8] P.K. Panda, Review: environmental friendly lead-free piezoelectric materials, J. Mater. Sci. 44 (2009) 5049.

[9] B. Parija, T. Badapanda, S. Panigrahi, T.P. Sinha, Ferroelectric and piezoelectric properties of (1-x)($Bi_{0.5}Na_{0.5}$)TiO_3-x$BaTiO_3$ ceramics, J. Mater. Sci.: Mater. Electron. 24 (2013) 402.

[10] R. Ranjan, A. Dviwedi, Structure and dielectric properties of $(Na_{0.50}Bi_{0.50})_{1-x}Ba_xTiO_3$: $0 \leq x \leq 0.10$, Solid State Commun. 135 (2005) 394.

[11] R. Potyrailo, K. Rajan, K. Stoewe, I. Takeuchi, B. Chisholm, H. Lam, Combinatorial and high-throughput screening of materials libraries: review of state of the art, ACS Comb. Sci. 13 (2011) 579.

[12] S. Guerin, B.E. Hayden, Physical vapor deposition method for the high-throughput synthesis of solid-state material libraries, J. Comb. Chem. 8 (2006) 66.

[13] M.S.B. Darby, S. Guerin, B.E. Hayden, H.-J. Schreiner, S. Yakovlev, High throughput physical vapour deposition and dielectric and ferroelectric screening of (Bi,Na)TiO_3 thin-film libraries, J. Appl. Phys. 113 (2013) 014104.

[14] P.S. Anderson, S. Guerin, B.E. Hayden, M.A. Khan, A.J. Bell, Y. Han, M. Pasha, K.R. Whittle, I.M. Reaney, Synthesis of the ferroelectric solid solution, $Pb(Zr_{1-x}Ti_x)O_3$ on a single substrate using a modified molecular beam epitaxy technique, Appl. Phys. Lett. 90 (2007) 202907.

[15] M. Mirsaneh, B.E. Hayden, S. Miao, J. Pokorny, S. Perini, E. Furman, M.T. Lanagan, R. Ubic, I.M. Reaney, High throughput synthesis and characterization of the $Pb_nNb_2O_{5+n}$ ($0.5<n<4.1$) system on a single chip, Acta Mater. 59 (2011) 2201.

[16] M. Mirsaneh, B.E. Hayden, E. Furman, S. Perini, M.T. Lanagan, I.M. Reaney, High dielectric tenability in lead niobate pyrochlore films, Appl. Phys. Lett. 100 (2012) 08901.

[17] M. Li, M.J. Pietrowski, R.A. De Souza, H. Zhang, I.M. Reaney, S.N. Cook, J.A. Kilner, D.C. Sinclair, A family of oxide ion conductors based on the ferroelectric perovskite $Na_{0.5}Bi_{0.5}TiO_3$, Nat. Mater.13 (2014) 31.

[18] T. Harigai, Y. Tanaka, H. Adachi, E. Fujii, Piezoelectric properties of lead-free $(Na,Bi)TiO_3$-$BaTiO_3$ (001) epitaxial thin films around the morphotropic phase boundary, Appl. Phys. Express 3 (2010) 111501.

[19]Y. Guo, D. Akai, K. Sawada, M. Ishida, Dielectric and ferroelectric properties of highly (100)-oriented $(Na_{0.5}Bi_{0.5})_{0.94}Ba_{0.06}TiO_3$ thin films grown on $LaNiO_3/\gamma$-Al_2O_3/Si substrate by chemical solution deposition, Solid State Sci. 10 (2008) 928.

[20] X. Liu, X.J. Zheng, J.Y. Liu, K.S. Zhou, D.H. Huang, Effect of annealing temperature on the electrostrictive properties of $0.94(Na_{0.5}Bi_{0.5})TiO_3$-$0.06BaTiO_3$ thin films, J. Electroceram. 29 (2012) 270.

[21] M. Cernea, L. Trupina, C. Dragoi, B.S. Vasile, R. Trusca, Structural and piezoelectric characteristics of BNT-$BT_{0.05}$ thin films processed by sol-gel technique, J. Alloys Comp. 515 (2012) 166.

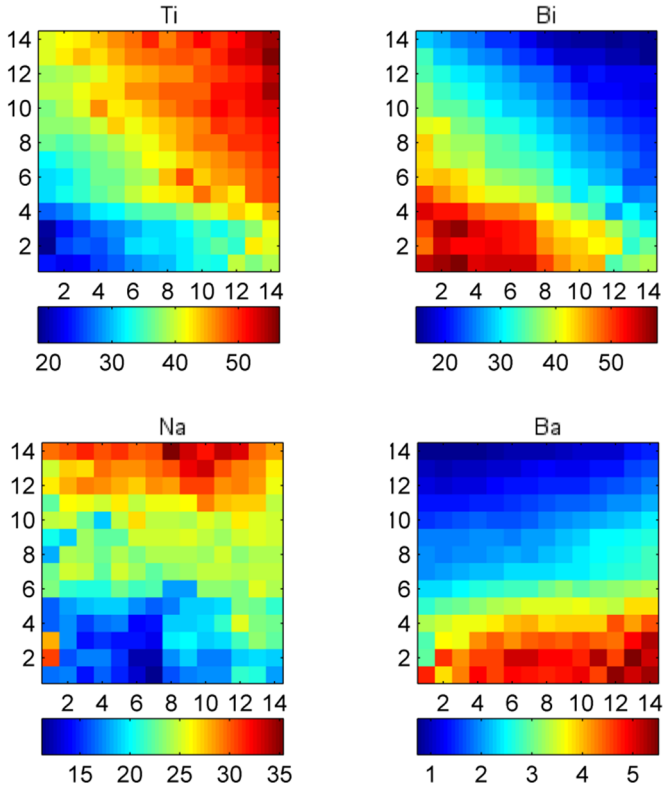

Fig. 1. Composition range of the Bi-Na-Ti-Ba-O thin-film materials library deposited for 1 hour (thickness 160-240 nm).

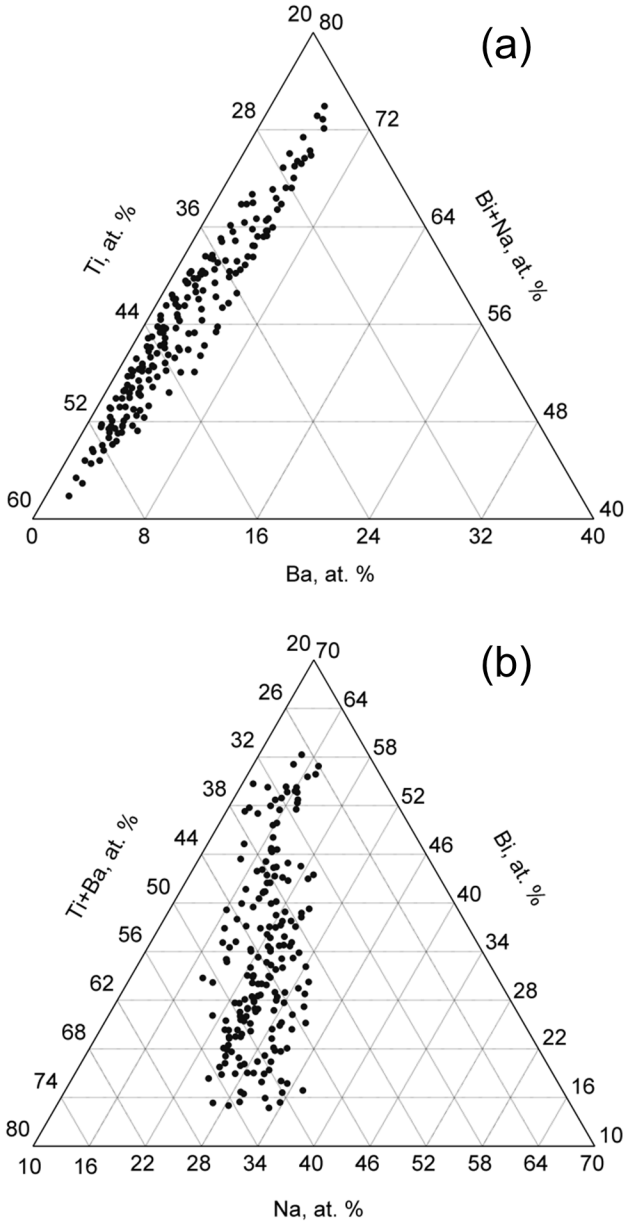

Fig. 2. Representation of the Bi-Na-Ti-Ba-O thin-film materials library in pseudo-ternary composition space by combining Bi and Na (a) and Ti and Ba (b).

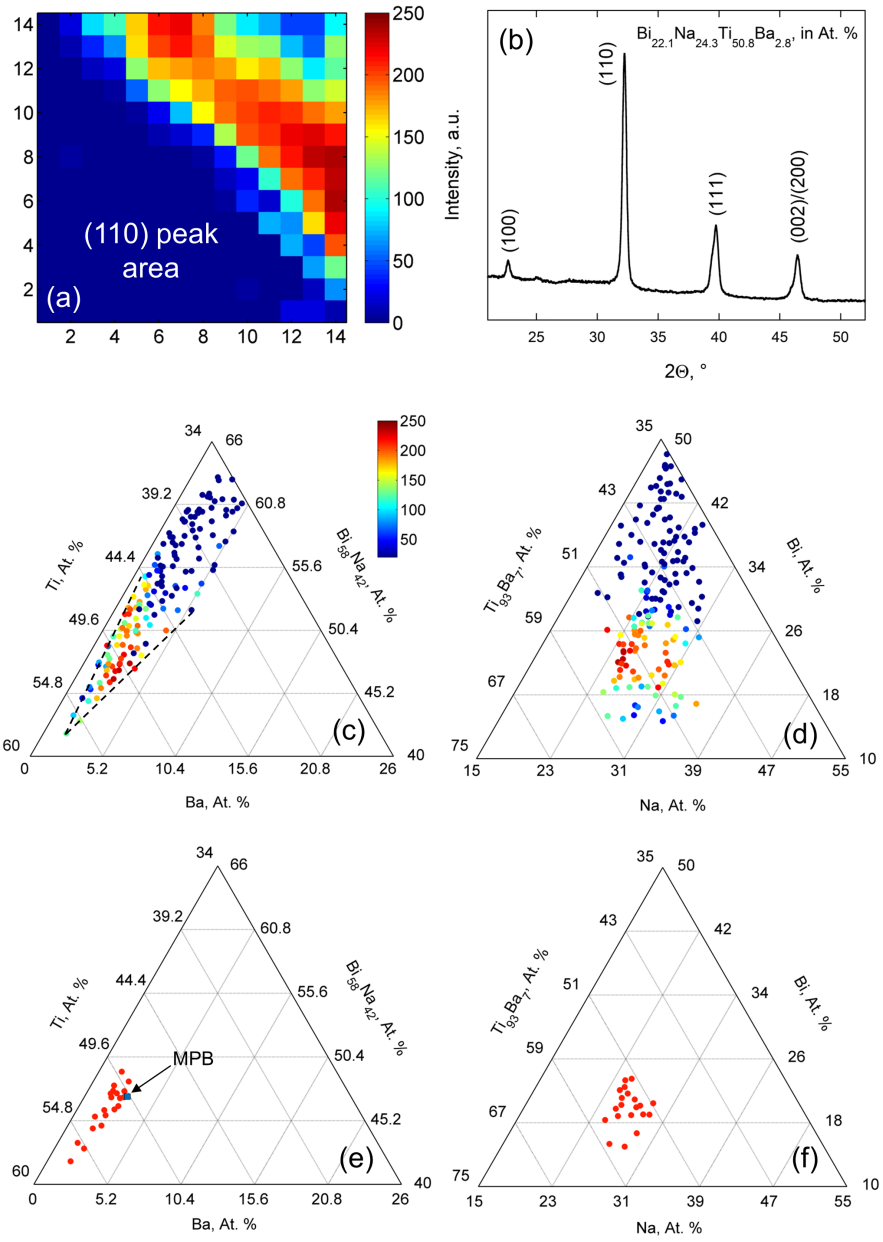

Fig. 3. Summary of screening of the perovskite phase in the Bi-Na-Ti-Ba-O thin-film materials library deposited for 1 hour and annealed at 700 °C for 30 min: on-chip distribution of the area under (110) perovskite pseudo-cubic peak (a), arbitrary units; selected XRD pattern corresponding to the composition $Bi_{22.1}Na_{24.3}Ti_{50.8}Ba_{2.8}$ (in At. % - close to the nominal MPB $0.94(Bi_{0.5}Na_{0.5})TiO_3$-$0.06BaTiO_3$) (b); area under (110) perovskite peak in pseudo-ternary composition space (c,d); area of the occurrence of pure perovskite phase in the investigated composition range (e,f). Dashed lines on (c) mark positions of the physical top and right edges of the materials library.

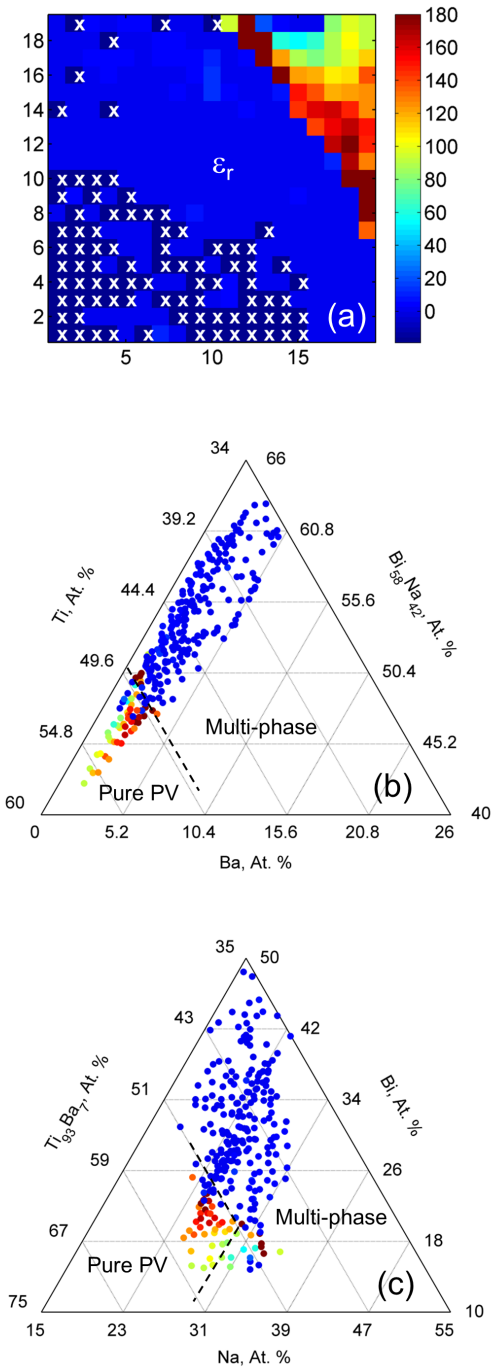

Fig. 4. Relative dielectric permittivity measured at room temperature, 1 kHz and 50 mV_{pp} for the Bi-Na-Ti-Ba-O thin-film materials library deposited for 1 hour and annealed at 700 °C for 30 min: on-chip (a) and in the pseudo-ternary composition space (b,c).

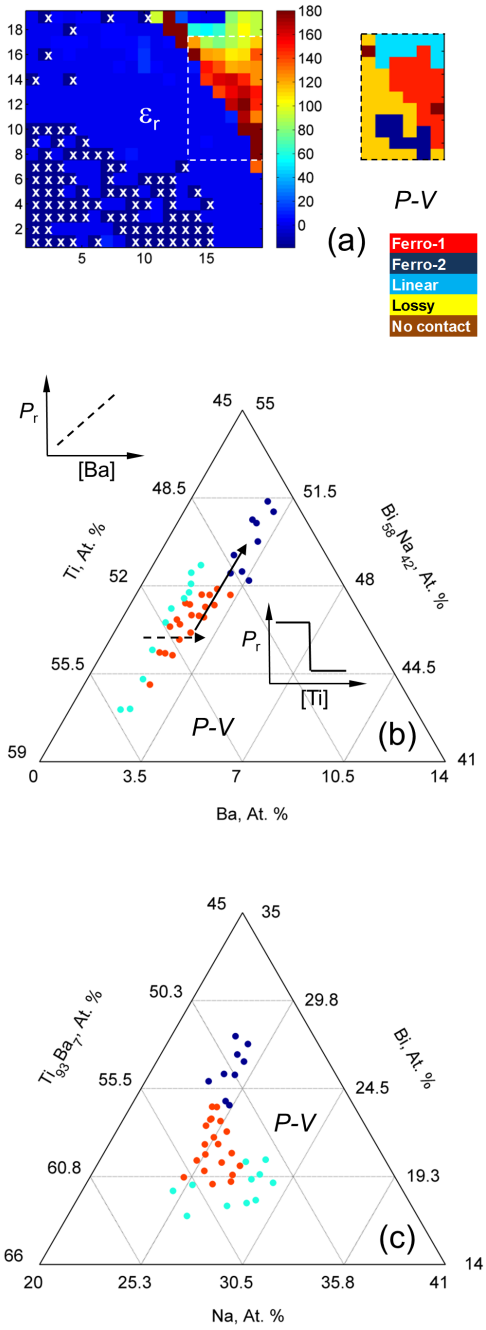

Fig. 5. Classification of the types of *P-V* characteristics observed for Bi-Na-Ti-Ba-O thin-film materials library after annealing at 700 °C for 30 min: on-chip locations of types of *P-V* curves (fragment encompassing ferroelectric phases) compared to the relative dielectric permittivity. Position of ferroelectric data section is delineated by the dashed lines (a). Positions of the ferroelectric and linear points of the materials library in pseudo-ternary composition space (b,c). Schematics on (b) depict trends in variation of the remnant polarization in the directions indicated by the arrows.

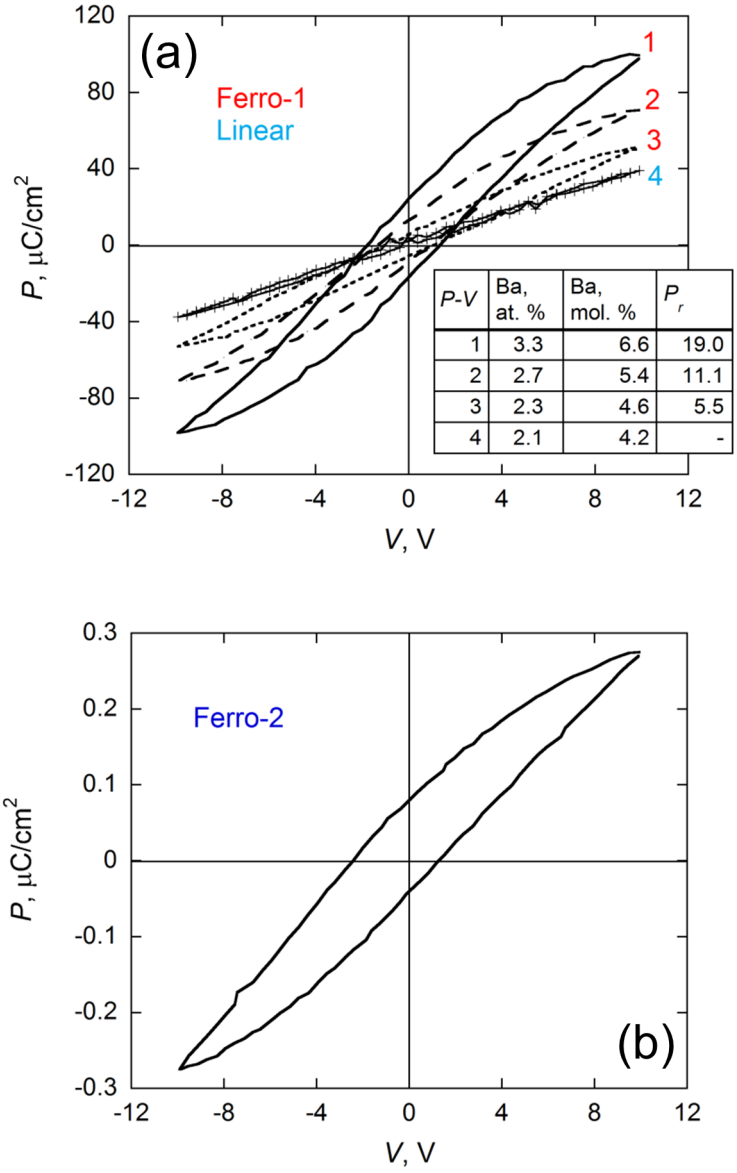

Fig. 6. *P-V* hysteresis loops obtained for representative compositions corresponding to "Ferro-1" (a) and "Ferro-2" (b) areas. Table on (a) summarizes remnant polarization measured for compounds with various Ba content and nearly equiatomic Bi/Na ratios. The compositions are: $Ti_{49.1}Bi_{23.4}Na_{24.2}Ba_{3.3}$ (1), $Ti_{49.4}Bi_{23.4}Na_{24.5}Ba_{2.7}$ (2), $Ti_{50.1}Bi_{21.9}Na_{25.7}Ba_{2.3}$ (3) and $Ti_{54.8}Bi_{18.4}Na_{24.7}Ba_{2.1}$ (4).

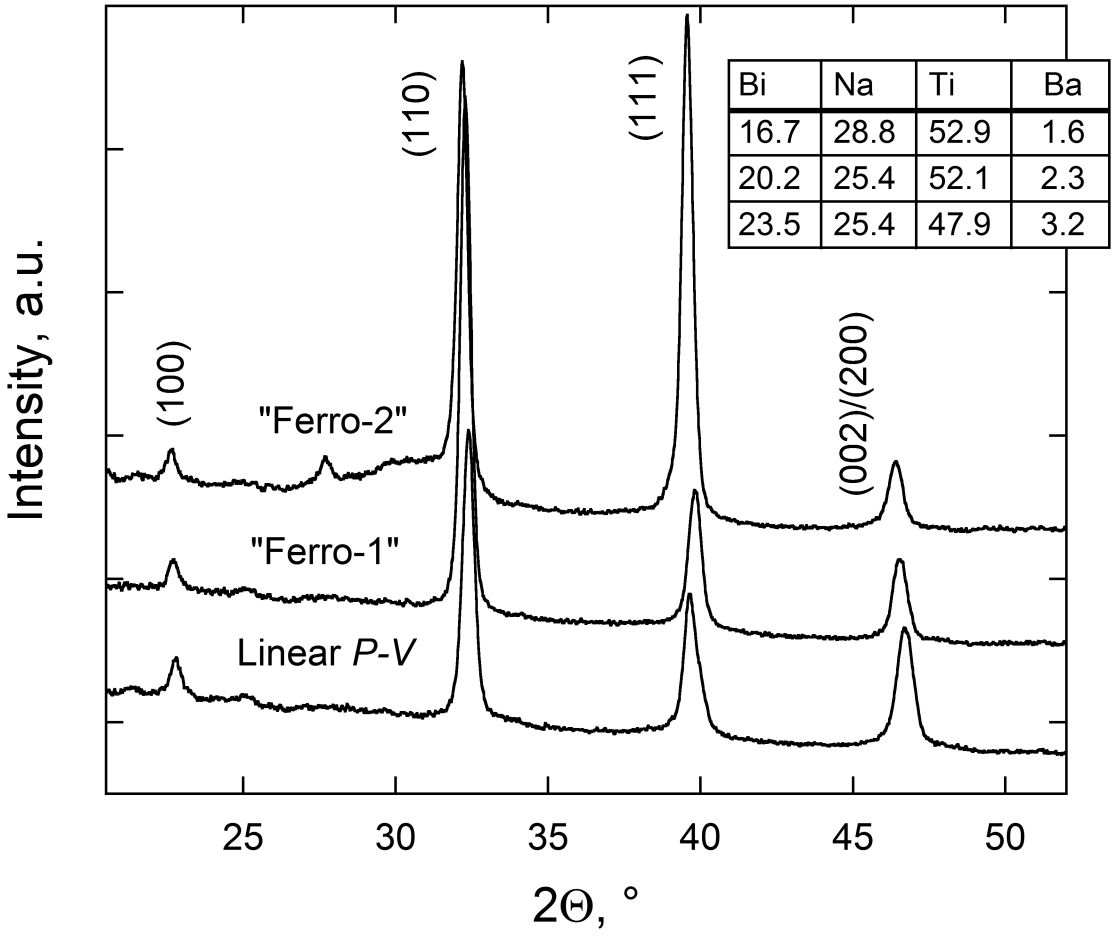

Fig. 7. X-ray diffraction patterns obtained for the linear, “Ferro-1” and “Ferro-2” regions of Bi-Na-Ti-Ba-O thin-film materials library. Table shows corresponding compositions in At. %.